

RESEARCH ARTICLE

Open Access



Prototheca spp. induce an inflammatory response via mtROS-mediated activation of NF- κ B and NLRP3 inflammasome pathways in bovine mammary epithelial cell cultures

Wenpeng Zhao¹, Fumeng He¹, Herman W. Barkema², Siyu Xu¹, Jian Gao¹, Gang Liu¹, Zhaoju Deng¹, Muhammad Shahid¹, Yuxiang Shi³, John P. Kastelic² and Bo Han^{1*} 

Abstract

Emergence of bovine mastitis caused by *Prototheca* algae is the impetus to better understand these infections. Both *P. bovis* and *P. ciferrii* belong to *Prototheca* algae, but they differ in their pathogenicity to induce inflammatory responses. The objective was to characterize and compare pathogenesis of inflammatory responses in bMECs induced by *P. bovis* versus *P. ciferrii*. Mitochondrial ultrastructure, activity and mtROS in bMECs were assessed with transmission electron microscopy and laser scanning confocal microscopy. Cytokines, including TNF- α , IL-1 β and IL-18, were measured by ELISA and real-time PCR, whereas expressions of various proteins in the NF- κ B and NLRP3 inflammasome pathways were detected with immunofluorescence or Western blot. Infection with *P. bovis* or *P. ciferrii* damaged mitochondria, including dissolution and vacuolation of cristae, and decreased mitochondrial activity, with *P. bovis* being more pathogenic and causing greater destruction. There were increases in NADPH production and mtROS accumulation in infected bMECs, with *P. bovis* causing greater increases and also inducing higher cytokine concentrations. Expressions of NF- κ B-p65, p-NF- κ B-p65, I κ B α and p-I κ B α proteins in the NF- κ B pathway, as well as NLRP3, Pro Caspase1, Caspase1 p20, ASC, Pro IL-1 β , and IL-1 β proteins in the NLRP3 inflammasome pathway, were significantly higher in *P. bovis*-infected bMECs. However, mito-TEMPO significantly inhibited production of cytokines and decreased expression of proteins in NF- κ B and NLRP3 inflammasome pathways in bMECs infected with either *P. bovis* or *P. ciferrii*. In conclusion, *P. bovis* or *P. ciferrii* infections induced inflammatory responses in bMECs, with increased mtROS in damaged mitochondria and activated NF- κ B and NLRP3 inflammasome pathways, with *P. bovis* causing a more severe reaction.

Keywords: *Prototheca* spp., bovine mammary epithelial cells, mtROS, NF- κ B/NLRP3 inflammasome pathway, inflammation

Introduction

Mastitis is common in dairy cattle worldwide, causing serious reductions in milk yield and quality and large financial losses [1, 2]. Infections with pathogens are an

important cause of mastitis. *Prototheca* spp. are unicellular achlorophyllous algae, 3–30 μ m in diameter, that lack a specific glucosamine cell wall or chloroplasts; specific species include *P. bovis*, *P. ciferrii*, *P. cerasi*, *P. pringsheimii*, *P. blaschkeae*, *P. wickerhamii*, *P. xanthoriae*, *P. cookie*, *P. xanthoriae*, *P. cutis*, *P. miyajii*, *P. tumulicola*, *P. moriformis*, *P. stagnora*, and *P. ulmea* [3–5]. Bovine mastitis caused by *Prototheca* spp. is characterized by an abrupt decrease in both milk production and quality,

*Correspondence: hanbo@cau.edu.cn

¹ Department of Clinical Veterinary Medicine, College of Veterinary Medicine, China Agricultural University, Beijing 100193, China
Full list of author information is available at the end of the article



© The Author(s) 2021. **Open Access** This article is licensed under a Creative Commons Attribution 4.0 International License, which permits use, sharing, adaptation, distribution and reproduction in any medium or format, as long as you give appropriate credit to the original author(s) and the source, provide a link to the Creative Commons licence, and indicate if changes were made. The images or other third party material in this article are included in the article's Creative Commons licence, unless indicated otherwise in a credit line to the material. If material is not included in the article's Creative Commons licence and your intended use is not permitted by statutory regulation or exceeds the permitted use, you will need to obtain permission directly from the copyright holder. To view a copy of this licence, visit <http://creativecommons.org/licenses/by/4.0/>. The Creative Commons Public Domain Dedication waiver (<http://creativecommons.org/publicdomain/zero/1.0/>) applies to the data made available in this article, unless otherwise stated in a credit line to the data.

an increased somatic cell count, and frequently culling, with substantial economic losses [6]. Among *Prototheca* spp., *P. bovis* was the causative pathogen of bovine mastitis, whereas *P. ciferrii* occasionally causes granulomatous lesions in experimentally infected bovine udders and protothecosis in humans [7, 8]. *Prototheca* spp. mastitis has been reported in many countries, including Canada, Poland, Italy, Brazil, and Japan [9–11].

An inflammatory response, a typical feature of bovine mastitis, is characterized by release of inflammatory cytokines such as IL-1 β , TNF- α and IL-18. Numerous signal molecules or pathways are involved in regulation of an inflammatory response, including reactive oxygen species, inflammasome and NF- κ B pathway [12, 13]. The inflammasome is an upstream regulatory mechanism that triggers an inflammatory response when stimulated by pathogens. The best characterized inflammasome is the NLRP3 inflammasome, comprised of NLRP3, apoptosis-associated speck-like protein containing adaptor (ASC), and Caspase1 [12–14]. Furthermore, NLRP3 is a cytosolic pattern recognition receptor (PRR) activated by pathogen-associated molecular patterns (PAMPs) and damage-associated molecular patterns (DAMPs) [15]. Once activated, the inflammasome recruits NLRP3, ASC, and Caspase1, and cleaves Pro Caspase1 to an active form (cleavage Caspase1) that triggers proteolytic cleavage of Pro IL-1 β and Pro IL-18 to mature and secreted forms [12, 15]. Although NLRP3 signaling usually confers protection, excessive activation can damage cells and cause inflammatory diseases [16–18]. The NLRP3 inflammasome can be generated and activated by *Escherichia coli* and *Staphylococcus aureus*, causing an aggravated inflammatory response and damage in bMECs [19, 20]. Activation of the NLRP3 inflammasome is regulated by various genes. In that regard, NF- κ B participates, and has an important regulatory role, in activation of the NLRP3 inflammasome, which triggers an inflammatory response [21]. Furthermore, an activated NF- κ B pathway could function as an upstream activator of NLRP3 and contribute to regulating inflammatory cytokines [22, 23].

Mitochondrial reactive oxygen species (mtROS) also activate the NLRP3 inflammasome, promoting inflammation and enhancing immune responses [24, 25]. Accumulation of damaged mitochondria may be essential for NLRP3 activation. In addition to increased mtROS, exposure of mitochondria-derived DAMPs (mtDAMPs) [e.g., mitochondrial DNA (mtDNA)] and cardiolipin to the cytosol, can also promote NLRP3 activation [26, 27]. Activation of the NLRP3 inflammasome has a crucial role in inflammatory responses in many diseases. Clinical bovine mastitis is usually characterized by pain, edema, cytokine production, and cellular infiltration. In *Prototheca* spp. mastitis, there are interstitial infiltrates

of macrophages, plasma cells and lymphocytes into the mammary gland, and an antiserum against bovine keratin had weak positive expression in damaged mammary tissue [28]. We reported that infections with *P. bovis* or *P. ciferrii* increased expression of cytokine mRNA in bMECs [29]; however, inflammatory responses in bovine mammary epithelial cells (bMECs) infected with *P. bovis* or *P. ciferrii* are not well characterized. Therefore, mitochondrial damage, inflammatory cytokines including TNF- α , IL-1 β and IL-18, and protein expression in the NF- κ B/NLRP3 pathway that regulate inflammation were measured to characterize and compare the pathogenesis of inflammatory responses in bMECs induced by infection with *P. bovis* versus *P. ciferrii*.

Materials and methods

Reagents and antibody

Cell Counting Kit-8 (CCK-8), NADP⁺/NADPH assay kit, Bicinchoninic acid (BCA) protein assay kit, radioimmunoprecipitation assay (RIPA) lysis buffer, Mito-Tracker Green staining solution and Hoechst 33342 live cell staining solution were purchased from Beyotime (Shanghai, China). ELISA assay kit was purchased from mlbio (Shanghai, China). 4', 6-Diamidino-2'-phenylindole dihydrochloride (DAPI), coverslips and Triton X-100, penicillin, streptomycin and bovine serum albumin (BSA) was purchased from Solarbio (Beijing, China). Enhanced chemiluminescence (ECL) kits were obtained from Thermo Fisher Scientific Pierce (Rockford, IL, USA). Fetal Bovine Serum (FBS) and Dulbecco's Modified Eagle's medium (DMEM) were purchased from Hyclone (Logan, UT, USA). Rotenone was purchased from MCE (Shanghai, China). Mito-SOX red mitochondrial superoxide indicator was purchased from Yeasen (Shanghai, China). Trizol Reagent, cDNA synthesis superMix and Two-step RT-PCR superMix were purchased from TransGen Biotech (Beijing, China). Primary antibodies, including NLRP3, ASC, Caspase-1, IL-1 β and α -Tubulin, were purchased from Proteintech (Wuhan, China), and NF- κ B p65, Phospho-NF- κ B p65, I κ B α and Phospho-I κ B α were purchased from Cell Signaling Technology (Danvers, MA, USA). Peroxidase-conjugated goat anti-mouse IgG and goat anti-rabbit IgG were purchased from Proteintech (Wuhan, China).

P. bovis and *P. ciferrii* isolates

Prototheca bovis was isolated in 2016 from 105 clinical mastitis milk samples collected on 6 large (> 500 cows) Chinese dairy farms, whereas the 58 *P. ciferrii* isolates were recovered in the same year from environmental samples from 3 large dairy farms, located in suburbs of Beijing, Tianjin and Shandong [3]. The isolates were stored at 4 °C at the College of Veterinary Medicine,

China Agricultural University, Beijing, China [3]. These *Prototheca* spp. were characterized as *P. bovis* and *P. ciferrii* by several methods. Firstly, based on cellular fatty acid pattern, *P. bovis* had more eicosadienoic acid (C20:2) compared to *P. ciferrii* [7]. Secondly, we determined 18S rDNA sequences using genotype-specific PCR. For this, a PCR mix (20 μ L) containing *Prototheca* (450 bp) fragment internal amplification control *Proto18-4f* (GACATGGCG AGGATTGACAGA) and *Proto18-4r* (AGCACACCC AATCGGTAGGA) primers (2.5 μ L each primer), DNA template (1 μ L), ddH₂O (4 μ L), and 2 \times EasyTaq PCR supermix (10 μ L) was amplified under specific conditions (2 min at 95 $^{\circ}$ C, followed by 34 cycles of 30 s at 95 $^{\circ}$ C, 30 s at 50 $^{\circ}$ C, and 30 s at 72 $^{\circ}$ C, with a final extension of 5 min at 72 $^{\circ}$ C). Amplified fragments were sent for sequencing (Sangon Biotech, Shanghai, China). Then, *P. bovis* and *P. ciferrii* were characterized by genotype-specific primers [3, 7]. Additionally, the *P. bovis* and *P. ciferrii* genotypes were further confirmed by restriction fragment length polymorphism analysis targeting the *cytb* gene fragment [7, 30]. Taken together, we confirmed *P. bovis* and *P. ciferrii* genotypes in the isolates recovered from clinical mastitis milk and environmental samples. These strains in within a species (*P. bovis* and *P. ciferrii*), strains had the same genotype, colony morphology and similar biochemical characteristics. We randomly selected 3 strains of each species for the following experiments, which were performed independently in triplicate. The 3 strains of *P. bovis* and 3 strains of *P. ciferrii* were isolated from clinical mastitis milk and environmental samples of 3 large farms located near suburbs of Beijing, Tianjin and Shandong, respectively [3]. Furthermore, within each species, genotype and colony morphology were the same and the biochemical characteristics were similar. Additionally, *P. ciferrii* grew more slowly than *P. bovis* on SDA and their colonies had differences in morphological characteristics; *P. ciferrii* produced small colonies with smooth surface and folded edges compared to *P. bovis*, whereas the latter had more eicosadienoic acid (C20:2) compared to the former [7]. *P. bovis* and *P. ciferrii* isolates were multiplied by streaking on sabouraud dextrose agar (SDA) and incubated at 37 $^{\circ}$ C for 48 h. Then, a single colony was placed in sabouraud dextrose broth (SDB) and incubated for 72 h. Thereafter, organisms were diluted in DMEM to achieve required concentrations.

Cell culture and treatment

The MAC-T line of bMECs (Shanghai Jingma Biological Technology Co., Ltd. China) was used for cell culture. bMECs were placed in DMEM medium supplemented with 10% fetal bovine serum, penicillin (100 U/mL) and streptomycin (100 U/mL) and grown in cell culture plates. Cells were incubated in 5% CO₂ at 37 $^{\circ}$ C, and cells

from passages 2–8 were used for experiments. Before infection, cells were put in 6-well plates (1 \times 10⁶ cells per well) and cultured overnight. Next, cells were infected with *P. bovis* or *P. ciferrii* at a 5:1 multiplicity of infection (MOI; ratio of *P. bovis* or *P. ciferrii* to bMECs) and incubated in 5% CO₂ at 37 $^{\circ}$ C for 12 h. Then, culture supernatants were collected and frozen (–80 $^{\circ}$ C) to subsequently determine cytokine concentrations, whereas cells were collected to extract and characterize proteins. Each experiment was conducted in triplicate.

Transmission electron microscopy

The bMECs were fixed as described [29] and transmission electron microscopy (TEM) used to assess ultrastructure. Briefly, cells were washed 3 times with phosphate buffered solution (PBS) and then fixed with 2.5% glutaraldehyde solution (pH 7.4) for 2–4 h at room temperature. After fixation, samples were routinely processed and examined with a transmission electron microscope (H7650, Hitachi, Tokyo, Japan) at an accelerating voltage of 80 kV.

Cell viability assay

Cell viability was measured with a Cell Counting Kit-8 (CCK-8). The bMECs were seeded into 96-well plates at a density of 5 \times 10³ cells/well, allowed to adhere overnight, and then treated for 12 h with various concentrations of rotenone (mitochondrial electron transport chain complex I inhibitor) used to enhance mitochondrial reactive oxygen species production (i.e., a positive control). Then, bMECs were washed 3 times with PBS and 10 μ L CCK-8 solution added to each well. After incubation for 1.5 h at 37 $^{\circ}$ C with 5% CO₂, OD values were read at 570 nm.

Mito-tracker green staining

The bMECs were cultured in 6-well plates overnight and then infected with *P. bovis* or *P. ciferrii* at a 5:1 MOI. After 12 h, bMECs were washed 3 times with PBS and 2 mL of warm (37 $^{\circ}$ C) Mito-Tracker Green staining solution was added. After incubation for 30 min at 37 $^{\circ}$ C, Mito-Tracker Green staining solution was removed and 2 mL fresh cell culture solution (37 $^{\circ}$ C) was added. Then, 10 μ L Hoechst 33342 live cell staining solution was added to each well. After incubating for 10 min at 37 $^{\circ}$ C, the dye-containing culture medium was aspirated, cells were washed 3 times with culture medium and observed with laser scanning confocal microscopy (Olympus-FV3000, Olympus, Tokyo, Japan).

Mitochondrial ROS measurement

To detect intracellular mtROS production, bMECs were seeded into 6-well plates with cell climbing films and infected with *P. bovis* or *P. ciferrii* at a 5:1 MOI. After

12 h, Mito-SOX red mitochondrial superoxide indicator was used to label mitochondrial reactive oxygen species. To induce accumulation of mtROS (positive control), bMECs were treated with 2.5 μM rotenone for 12 h. Next, cells were incubated with Mito-SOX (5 μM) in the dark for 10 min at 37 °C and then washed 3 times with PBS. Nuclei were stained with 300 nM 4,6-diamino-2-phenyl indole (DAPI) for 5 min at 37 °C and washed with PBS. Slides were covered with glass cover slips and intracellular mtROS assessed with laser scanning confocal microscopy (Olympus-FV3000).

NADPH analysis

The bMECs were cultured into 6-well plates overnight and then infected with *P. bovis* or *P. ciferrii* at a 5:1 MOI for 12 h. The NADPH content in cells was determined with a commercial NADP+/NADPH Assay Kit, according to the manufacturer’s protocol. Briefly, 200 μL NADP+/NADPH extract was added into each hole of the 6-well plate, gently blown to promote cell lysis, and supernatant collected for subsequent experiments. Then, 50 μL supernatant and 200 μL of G6PDH working solution were added into each 96-well plate. After incubation for 10 min at 37 °C, 10 μL chromogenic solution was added into each well and after incubation for 20 min at 37 °C, absorbance was measured at 450 nm.

ELISA

The bMECs were infected with the 3 *P. bovis* or 3 *P. ciferrii* isolates at a 5:1 MOI for 12 h, and 10 μM of 2-(2,2,6,6-Tetramethylpiperidin-1-oxyl-4-ylamino)-2-oxoethyl triphenyl-phosphonium chloride, monohydrate (mito-TEMPO), a mitochondria-targeted superoxide dismutase mimetic with superoxide and alkyl radical scavenging properties, was used to scavenge superoxide. Cytokines in supernatants of bMECs culture medium were quantified by ELISA kits, according to the manufacturer’s instructions. Cell culture supernatants were collected and concentrations of TNF-α, IL-1β and IL-18 in supernatants were measured, based on OD values at 450 nm.

RNA extraction and real time PCR

The bMECs were treated as described above for ELISA, washed 3 times with PBS, and cells collected for total RNA extraction. Trizol Reagent was pre-chilled on ice and 1 mL added to cell samples for 5 min to lyse cells. Mixed liquid was centrifuged at 12 000 × g for 15 min at 4 °C and supernatant collected. Total mRNA of bMECs was extracted with mRNA extraction kit according to manufacturer’s instructions. Relative expression levels of TNF-α, IL-1β and IL-18 mRNA were determined using the StepOnePlus Real-Time PCR systems. Data were

analyzed according to the 2^{-ΔΔCt} method and results were expressed as relative mRNA levels [7]. Primer sequences for GAPDH (housekeeping gene), TNF-α, IL-1β, and IL-18 are presented in Table 1.

Immunofluorescence

The bMECs were treated as described above for ELISA, washed 3 times with PBS and then fixed in 4% paraformaldehyde for 30 min and subsequently permeabilized in 0.25% Triton X-100. Cells were incubated with 3% bovine serum for 30 min at room temperature and then incubated overnight at 4 °C with the following primary antibodies: NLRP3, NF-κB p65, Phospho-NF-κB p65, ASC, and IL-1β. Next, samples were washed with PBS and incubated with Alexa Fluor 488-labeled goat anti-rabbit IgG (H+L) for 1 h at room temperature. Then, samples were washed with PBS and stained with DAPI for 20 min. After washing with PBS, slides were covered with glass cover slips and observed under a laser scanning confocal microscope (Olympus-FV3000).

Western blot

The bMECs were treated as described above for ELISA and then lysed on ice and the cell lysate suspension collected and centrifuged (12 000 × g, 4 °C) for 15 min. Total protein concentration in the supernatant was determined with a BCA protein assay kit. Protein samples were denatured in boiling water for 10 min and then separated by SDS-PAGE and transferred onto polyvinylidene difluoride (PVDF) membranes. These membranes were blocked with 5% nonfat dry milk for 2 h at room temperature, then incubated overnight at 4 °C with the following primary antibodies: α-Tubulin, NLRP3, NF-κB p65, Phospho-NF-κB p65, IκBα, Phospho-IκBα, ASC, Caspase-1, and IL-1β. For α-Tubulin, membranes were incubated with mouse anti-α-Tubulin antibody, whereas for all other proteins, they were incubated with secondary antibody against rabbit IgG for 1 h at room temperature. After washing with Tris-buffered saline, the membrane was developed using ECL reagents and visualized with a

Table 1 List of primers for real-time PCR.

Gene	Primer	Sequence (5'-3')	Size (bp)
GAPDH	Forward	TCACCAACTGGGACGACA	206
	Reverse	GCATACAGGGACAGCACA	
TNF-α	Forward	ATGTGTGTGGAGAGCGTCAA	145
	Reverse	GGGCCATACAGCTCCACAAA	
IL-1β	Forward	ATGACTTCCAAGCTGGCTGTTG	114
	Reverse	TTGATAAATTTGGGGTGGAAAAG	
IL-18	Forward	TTGCATCAGCTTTGTGGAAA	213
	Reverse	TGGGGTGCATTATCTGAACA	

chemiluminescence system. Results were normalized to α -Tubulin, and band density was analyzed with Image J (National Institutes of Health, Bethesda, MD, USA).

Statistical analyses

After visually confirming that the data were normally distributed, independent Student's *t*-tests or one-way ANOVA were used to analyze effects of *Prototheca* spp. on cell viability, NADPH content, inflammatory cytokines including TNF- α , IL-1 β and IL-18, and protein expression in NF- κ B/NLRP3 pathway, with a Bonferroni method used to correct multiple comparisons, $P < 0.05$ was divided by the number of tests to be considered statistically significant. Data are reported as means \pm standard deviation (SD) of 3 independent experiments (3 technical replicates were carried out in each experiment).

Results

Prototheca spp. infection caused mitochondrial damage in bMECs

In uninfected bMECs (controls), mitochondria had reticulated morphologies and mitochondrial cristae were clearly visible with TEM (Figure 1, panels A1 and A2), whereas in bMECs infected with *P. ciferrii*, mitochondria had relatively minor damage, including slight vacuolization (Figure 1, panels B1 and B2). In contrast, in bMECs infected with *P. bovis*, mitochondria had dissolution

of their cristae and large areas of vacuolation (Figure 1, panels C1 and C2). Intensity of green fluorescence was profoundly decreased in bMECs infected with *P. bovis*, with less suppression in the *P. ciferrii* infection group, although both were lower than the control (Figure 2), indicating decreased mitochondrial activity in infected bMECs. Both *P. bovis* and *P. ciferrii* induced mitochondrial damage, with more severe damage caused by *P. bovis*.

Prototheca spp. infection enhanced mtROS accumulation in bMECs

In bMECs infected with *P. ciferrii*, the mtROS assay had weak red fluorescence (Figure 3A). As a positive control, bMECs were treated with various concentrations of rotenone, with 2.5 μ M rotenone used to treat bMECs (Figure 3B). However, strong red fluorescence was observed in bMECs infected with *P. bovis* or treated with rotenone (Figure 3A); therefore, *P. bovis* induced greater mtROS accumulation. Furthermore, NADPH content was higher in bMECs infected with *P. bovis* or *P. ciferrii* compared to the control ($P < 0.05$), with the highest NADPH in the *P. bovis* infection group (Figure 3C). *P. bovis* and *P. ciferrii* decreased bMECs viability at 12 h post infection, although *P. bovis* caused a more profound decrease than *P. ciferrii* in the viability of bMECs (Figure 3D).

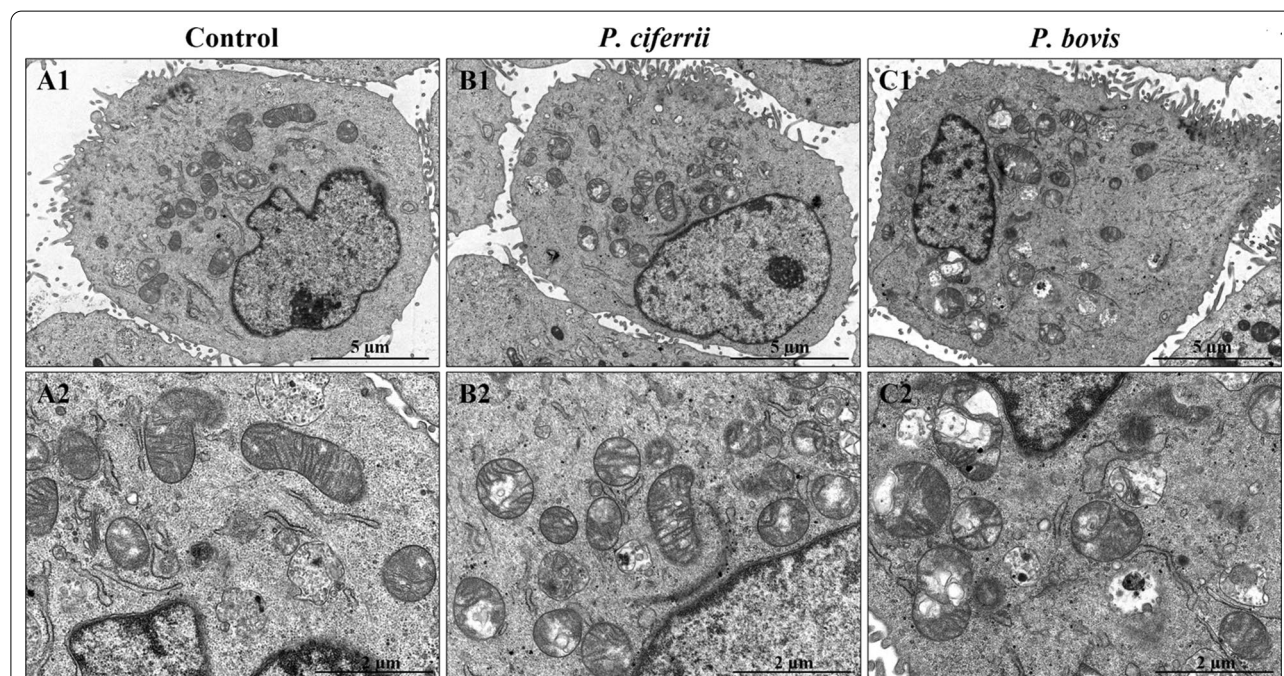


Figure 1 Mitochondrial ultrastructure in bMECs. **A1** and **A2**: Control group, with normal mitochondria and mitochondrial cristae in the bMECs. **B1** and **B2**: *P. ciferrii* infection group; note the slight vacuolization in mitochondria in *P. ciferrii*-infected bMECs. **C1** and **C2**: *P. bovis* infection group; note the mitochondrial cristae dissolution and large areas of vacuolation in bMECs.

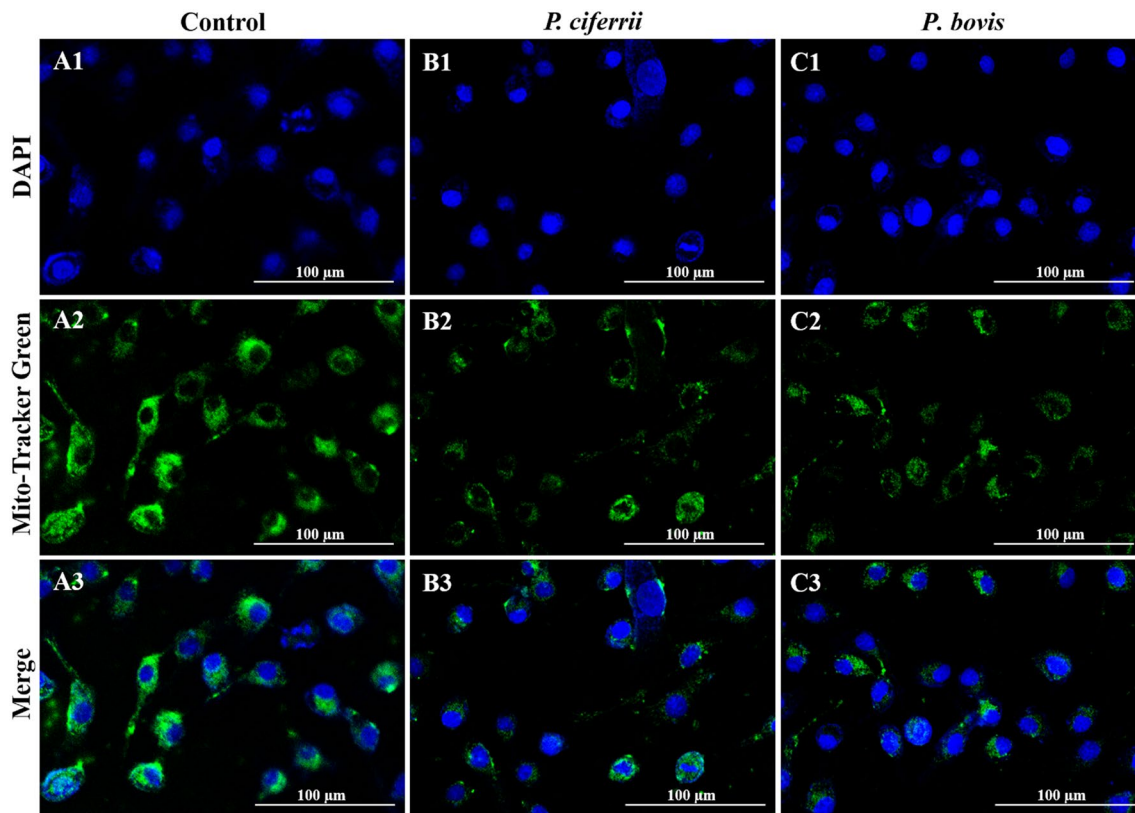


Figure 2 Mitochondrial activity in bMECs. Mito-Tracker Green is a mitochondrial green fluorescent probe, with intensity of green fluorescence reflecting mitochondrial activity. **A1, A2, and A3:** In the Control group, mitochondria in normal bMECs had strong green fluorescence, indicating good mitochondrial activity. **B1, B2, and B3:** In the *P. ciferrii* infection group, there was weak green fluorescence, indicating decreased mitochondrial activity in bMECs. **C1, C2, and C3:** In the *P. bovis* infection group, there was weak green fluorescence in bMECs, indicating mitochondrial activities were decreased.

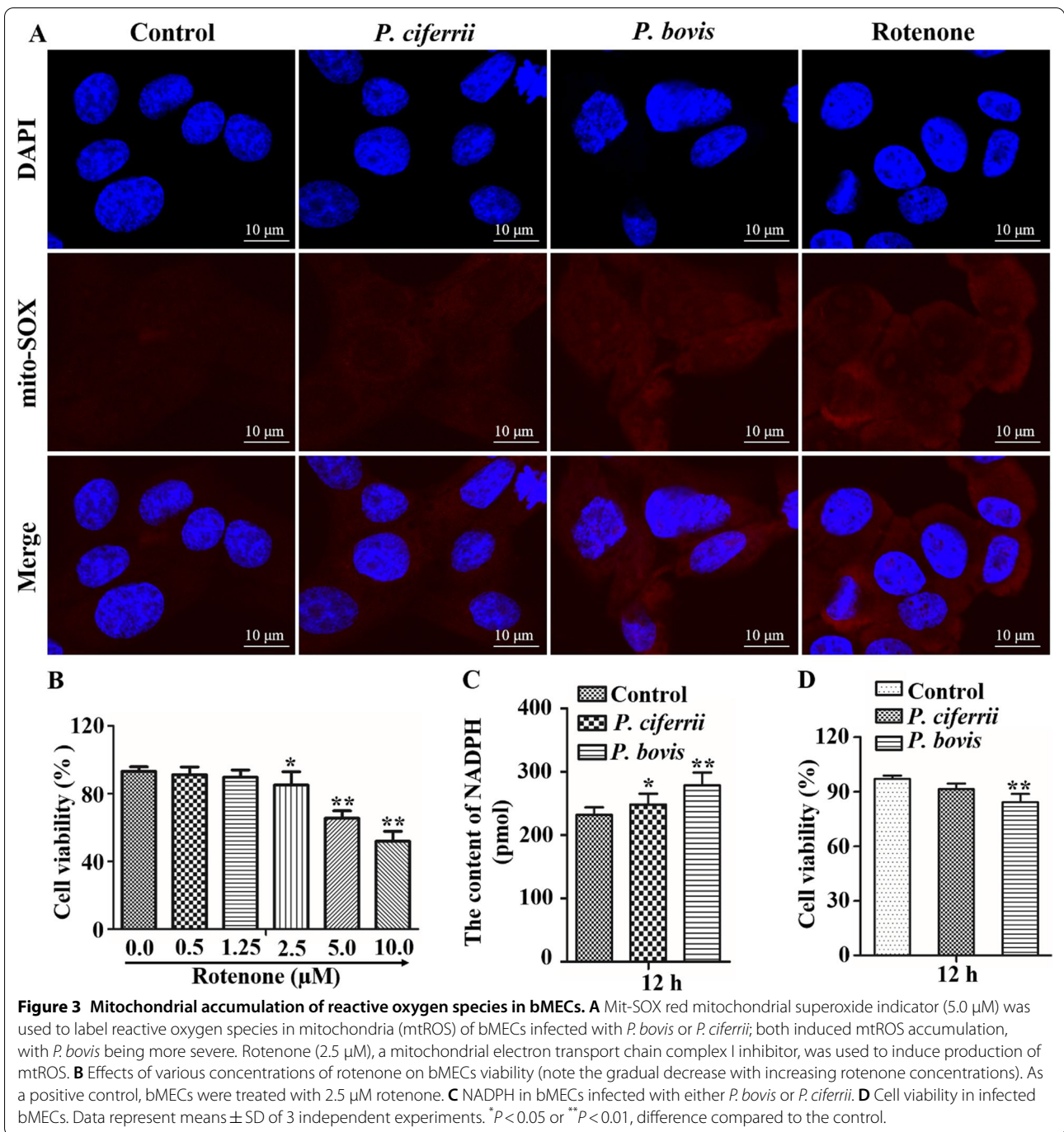
Prototheca spp. infection increased production of TNF- α , IL-1 β and IL-18 in bMECs

Infection with *P. ciferrii* increased production of IL-1 β , and IL-18 proteins and mRNAs in bMECs ($P < 0.05$), with more profound increases in bMECs infected with *P. bovis* ($P < 0.05$) (Figures 4B and C). *P. bovis* infection increased production of TNF- α proteins and mRNAs in bMECs ($P < 0.05$) (Figure 4A). In contrast, treatment with mito-TEMPO inhibited production of TNF- α , IL-1 β and IL-18 proteins and mRNAs in bMECs infected with *P. bovis* or *P. ciferrii* ($P < 0.05$) (Figures 4A, B and C). Expression of TNF- α , IL-1 β and IL-18 was not significantly different among isolates within *P. bovis* nor among *P. ciferrii* species (Additional file 1).

Prototheca spp. infection promoted protein expression of NF- κ B pathway in bMECs

Infection with *P. bovis* increased the green fluorescence intensity of NF- κ B p65 and p-NF- κ B p65 in bMECs (Figures 5A and B). Furthermore, in Western blots,

protein expression levels of NF- κ B p65 and p-NF- κ B p65 were also upregulated in *P. bovis*-infected bMECs ($P < 0.05$) compared to the control (Figures 5C, D and E). Although *P. ciferrii* infection in bMECs also increased expression levels of NF- κ B p65 and p-NF- κ B p65 proteins, changes were less profound than in the *P. bovis* infection group, with the immunofluorescence consistent with the Western blot (Figures 5A, B, C, D and E). In addition, expression level of p-I κ B α proteins was upregulated in *P. bovis*-infected cells ($P < 0.05$); there were fewer profound increases induced by *P. ciferrii*, but p-I κ B α ($P > 0.05$) was higher than the control (Figures 5C and G). Mito-TEMPO inhibited expression levels of NF- κ B p65 and p-NF- κ B p65 proteins in bMECs infected with *P. bovis* or *P. ciferrii* ($P < 0.05$) (Figures 5C, D and E). A similar trend in expression levels of I κ B α and p-I κ B α protein in bMECs infected with *P. bovis* or *P. ciferrii* was also observed after treatment with mito-TEMPO, but I κ B α and p-I κ B α were decreased compared to the *P. bovis* group ($P < 0.05$) (Figures 5C, F and G). Protein expression in the NF- κ B

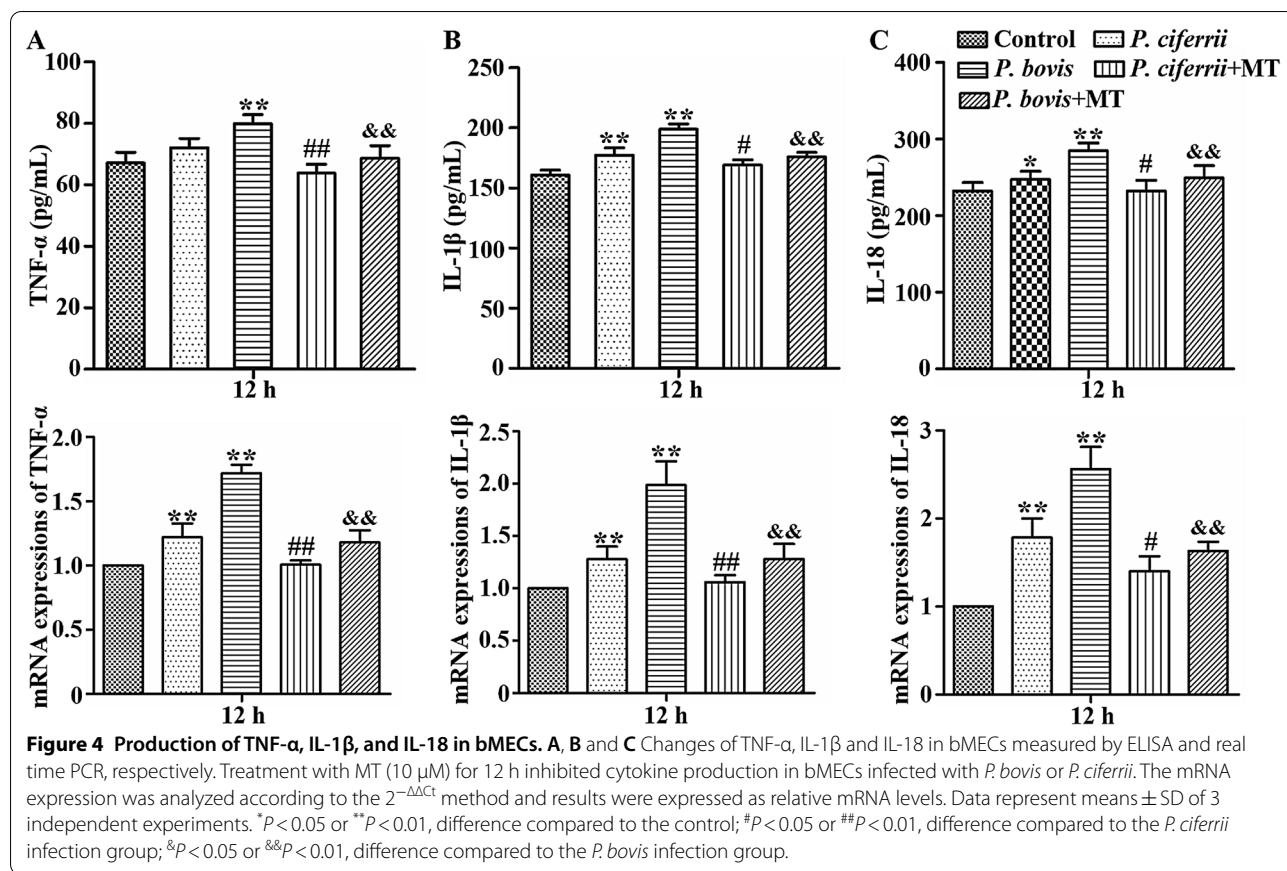


pathway was not significantly different among isolates within *P. bovis* or *P. ciferrii* species (Additional file 2).

Prototheca spp. infection contributed to NLRP3 inflammasome activation in bMECs

The green fluorescence intensity of NLRP3 and ASC was higher after infection with *P. bovis* or *P. ciferrii* compared to the control (Figures 6A and B). In contrast,

treatment with mito-TEMPO decreased the green fluorescence intensity of NLRP3 and ASC compared to infection with either *P. bovis* or *P. ciferrii* (Figures 6A and B). Furthermore, expression levels of NLRP3, Pro Caspase1, Caspase1 p20, and ASC proteins were upregulated in *P. bovis*-infected cells ($P < 0.05$) compared to the control (Figures 6C, D, E, F and G). Infection of bMECs with *P. ciferrii* also increased expression of these proteins, but



there was no significant change compared to the control (lowest $P=0.14$) (Figures 6C, D, E, F and G). Expression of these proteins were all upregulated after *P. bovis* or *P. ciferrii* infections, with more pronounced increases for *P. bovis*. However, in bMECs pretreated with mito-TEMPO, expression of NLRP3, Pro Caspase1, Caspase1 p20, and ASC proteins were inhibited in bMECs infected with *P. ciferrii* and *P. bovis* (except ASC, $P < 0.05$) (Figures 6C, D, E, F and G). Protein expression in NLRP3 inflammasome pathway was not significantly different among isolates within *P. bovis* or *P. ciferrii* species (Additional file 2).

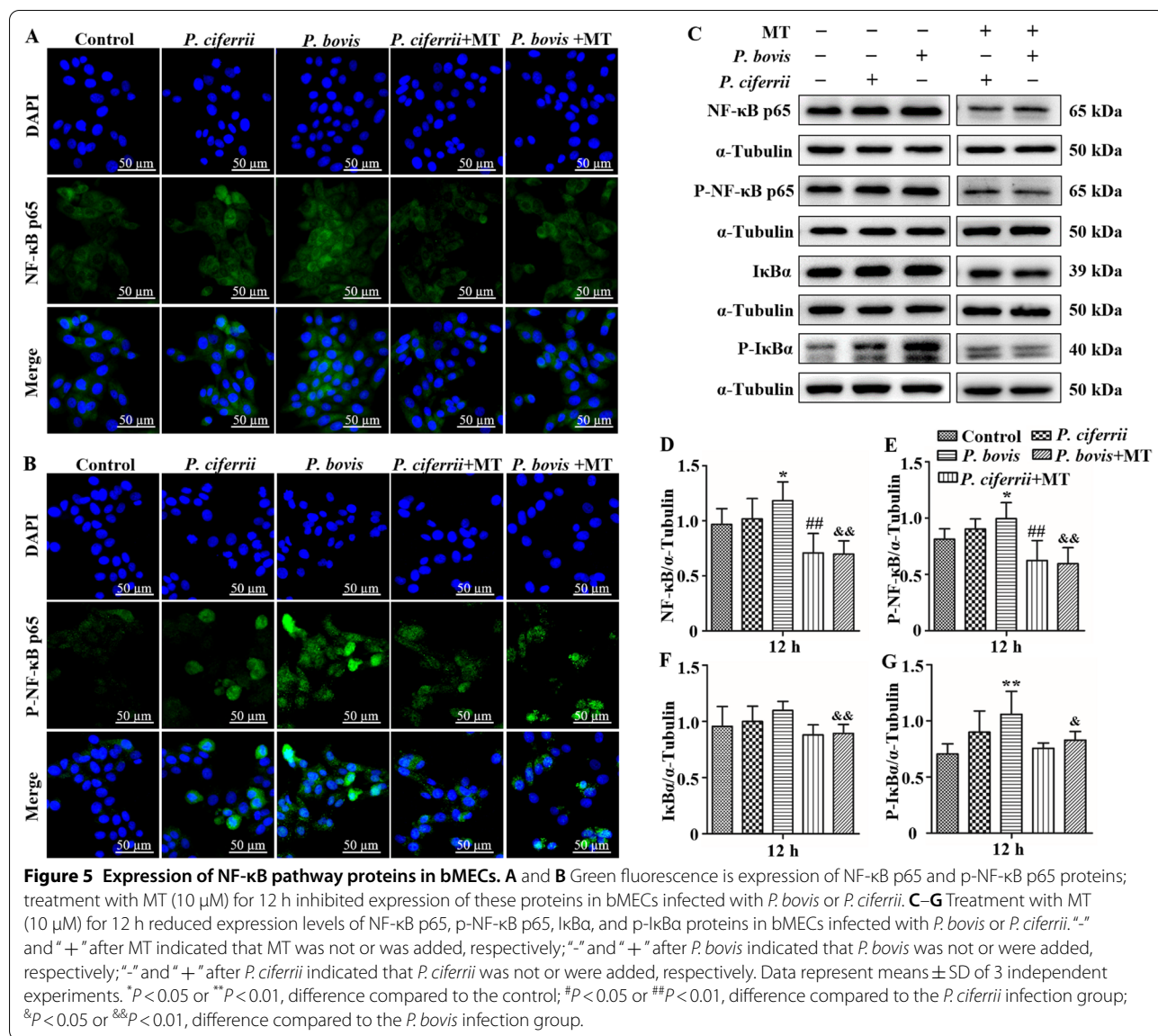
Prototheca spp. infection enhanced protein expression of IL-1 β in bMECs

Infection with *P. bovis* or *P. ciferrii* increased the red fluorescence intensity of IL-1 β in bMECs compared to the control (Figure 7A). However, treatment with mito-TEMPO decreased the red fluorescence intensity of IL-1 β in bMECs infected with *P. bovis* or *P. ciferrii* (Figure 7A). Furthermore, expression of Pro IL-1 β protein was upregulated in bMECs infected with *P. bovis* ($P < 0.05$) (Figures 7B and C). In addition, IL-1 β protein was also upregulated in bMECs infected with *P. bovis* or *P. ciferrii* ($P < 0.05$) (Figures 7B and D). Expression of

Pro IL-1 β and IL-1 β proteins were higher after *P. bovis* compared to *P. ciferrii* infection. Treatment with mito-TEMPO inhibited expression of Pro IL-1 β after *P. bovis* infection ($P < 0.05$) and IL-1 β protein in *P. bovis* and *P. ciferrii* infected bMECs were downregulated ($P < 0.05$) (Figures 7B, C and D). Protein expression of IL-1 β was not significantly different among isolates within *P. bovis* or *P. ciferrii* species (Additional file 2).

Discussion

In this study, *Prototheca* spp. infection in bMECs induced an inflammatory response through the NF- κ B and NLRP3 inflammasome pathways. Infection of bMECs with *Prototheca* spp., especially *P. bovis*, damaged mitochondria and promoted mtROS accumulation, which activated an inflammatory response through the NF- κ B and NLRP3 inflammasome pathways and enhanced IL-1 β production. However, scavenging mtROS decreased expressions of proteins in NF- κ B/NLRP3 inflammasome pathways and IL-1 β production in bMECs infected with *P. bovis* or *P. ciferrii*. Accumulation of mtROS may be important in inflammatory responses to *P. bovis* or *P. ciferrii* infections. Furthermore, mtROS activated NF- κ B/

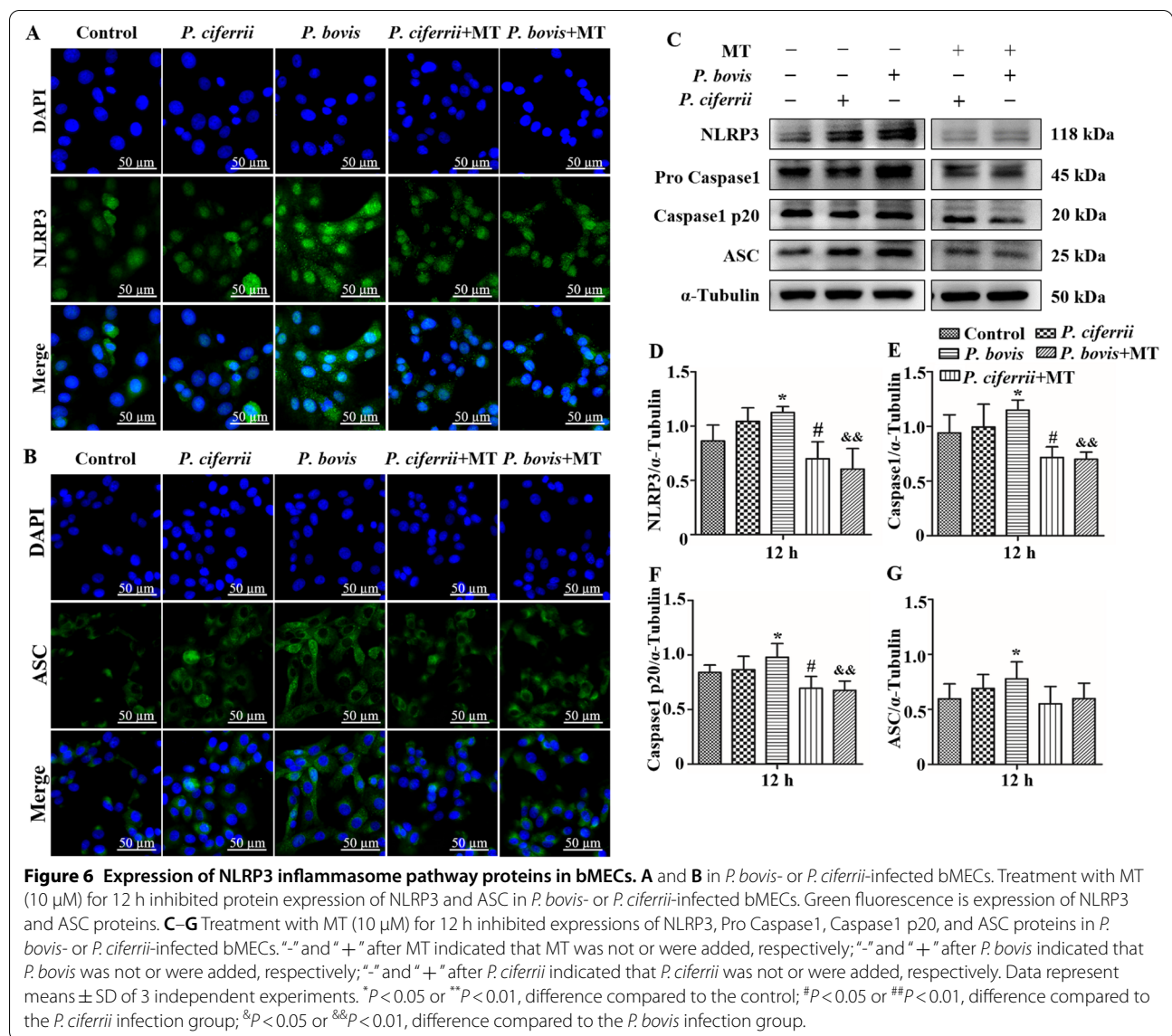


NLRP3 inflammasome pathways were involved in inflammation in bMECs infected with *P. bovis* and *P. ciferrii*.

Pathogenic infections can cause mitochondrial damage, including swelling and vacuolation, increase ROS, decrease membrane potential, and increase oxidative stress, both in vitro and in vivo [31–33]. Mitochondrial damage is closely related to development of inflammatory diseases [34]. In the current study, *Prototheca* spp. infections in bMECs, especially *P. bovis*, caused dissolution and large area vacuolation of mitochondrial cristae, and decreased mitochondrial activity. Mitochondria are the main site for mtROS production [35] and mitochondrial damage may contribute to mtROS production. Based on Mito-SOX, mtROS in bMECs increased after infection with *P. bovis*, with a lesser increase in *P.*

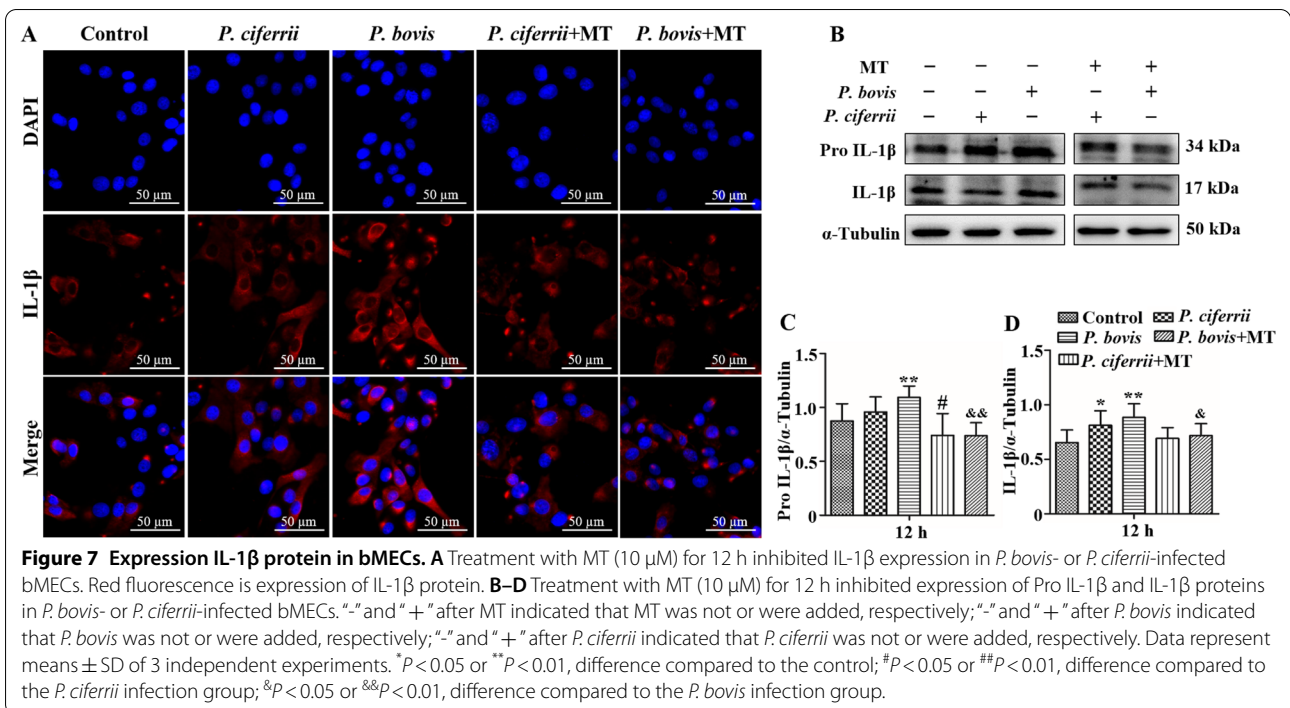
ciferrii-infected bMECs. NADPH is closely linked to ROS production and there is increasing evidence that increases in both ROS production and expression of NADPH oxidase were upregulated both in vitro and in vivo [36, 37]. In the present study, *P. bovis* or *P. ciferrii* infections in bMECs increased NADPH, which also provided evidence for production of mtROS. In this study, although strains for each species (*P. bovis* and *P. ciferrii*) were isolated from different samples, the pathogenicity of strains in each species to bMECs was similar, as both *P. bovis* and *P. ciferrii* induced mitochondrial damage and mtROS accumulation, with the former causing more profound damage.

Increased mitochondrial ROS promoted inflammatory responses in peritoneal mesothelial cells, macrophages



and T cells [15, 38]. Infection of bMECs with *P. bovis* or *P. ciferrii* stimulated inflammatory responses, characterized by release of inflammatory cytokines which activate immune effector cells to eliminate invading pathogens. There were significant increases in production of TNF- α , IL-18, and IL-1 β at 12 h after bMECs were infected with *P. bovis* or *P. ciferrii*, indicating a marked inflammatory response. However, responses to *P. bovis* were more severe than *P. ciferrii*, consistent with its greater pathogenicity. However, scavenging mtROS with mito-TEMPO significantly decreased cytokine production. Therefore, we inferred that infection with *P. bovis* or *P. ciferrii* induced inflammatory responses in bMECs that were mitigated by suppression of mtROS.

Inflammatory responses have many regulatory mechanisms, including the NF- κ B and NLRP3 inflammasome pathways [39, 40]. In the NF- κ B pathway, both I κ B α and NF- κ B p65 are inactive in the cytoplasm [41, 42]. However, when an upstream signal activates inhibitor of nuclear factor kappa-B kinase (IKK), it will be ubiquitinated, phosphorylated and degrade I κ B α , so that NF- κ B p65 will be activated and translocated from the cytoplasm to the nucleus to bind to the corresponding inflammation-related genes, promote transcription of inflammatory cytokines, and induce inflammation [42, 43]. In the current study, infection of bMECs with *P. bovis* or *P. ciferrii* activated the NF- κ B pathway, upregulating expression of I κ B α and NF- κ B p65 proteins. Furthermore, expression levels of phosphorylated I κ B α and



NF- κ B p65 proteins were upregulated after *P. bovis* or *P. ciferrii* infection, with greater upregulation of protein expression in the NF- κ B pathway induced by *P. bovis*, indicating higher pathogenicity. Activation of the NF- κ B pathway promoted inflammation, including a massive increase in cytokine production. In addition, mtROS activation of the IKK complex and subsequent signaling through the NF- κ B pathway led to secretion of pro-inflammatory cytokines by inducing the intermolecular disulfide linkage of nuclear factor κ B α essential modulator [44], whereas quenching mtROS in vivo decreased the NF- κ B-guided anti-inflammatory phenotype [45]. In the present study, in bMECs infected with *P. bovis* or *P. ciferrii*, mito-TEMPO decreased expression of various proteins in the NF- κ B pathway, including κ B α , NF- κ B p65, p- κ B α and p-NF- κ B p65. Thus, infection of bMECs with *Prototheca* spp., especially *P. bovis*, caused overexpression of proteins in the NF- κ B pathway and enhanced inflammatory responses through generation of mtROS.

Activation of inflammasomes is critical in inflammatory responses, with key roles in regulating inflammation caused by pathogenic bacteria [46, 47]. The NLRP3 inflammasome is well characterized [48]. Once activated, ASC self assembles and activates Pro Caspase1; the activated Caspase1 induces maturation of IL-1 β and IL-18 for subsequent release [48, 49]. Activation of the NLRP3 inflammasome is regulated by many factors, including bacterial infections and mtROS [50, 51]. In the present study, *P. bovis* or *P. ciferrii* infection in bMECs promoted

activation of NLRP3 inflammasomes to varying degrees, modulating upregulation of expression of NLRP3, ASC, and Caspase1 proteins, and promoting cleavage of Caspase1. We inferred that infection with either *P. bovis* or *P. ciferrii* contributed to the assembly of ASC, Pro Caspase1, and NLRP3 during inflammasome formation. Although *P. bovis* or *P. ciferrii* infections in bMECs promoted NLRP3 inflammasome activation, *P. bovis* induced larger increases in proteins of the NLRP3 inflammasome, indicating greater pathogenicity. Furthermore, expression levels of proteins of the downstream genes Pro IL-1 β and IL-1 β were upregulated in cells infected with *P. bovis* or *P. ciferrii*, although *P. bovis* caused more pronounced increases. Therefore, *P. bovis* induced a greater inflammatory response than *P. ciferrii* via the NLRP3 inflammasome pathway.

Generation of mtROS is one of the first identified triggers of NLRP3 inflammasome activation, although mtROS-independent activation of the NLRP3 inflammasome has been reported [52, 53]. In the present study, *P. bovis* or *P. ciferrii* infections induced mtROS in bMECs. However, treatment with mito-TEMPO downregulated expression levels of NLRP3, ASC and Caspase1 proteins in bMECs infected with *P. bovis* or *P. ciferrii*, whereas expression of Pro IL-1 β and IL-1 β proteins was also downregulated. Therefore, we inferred that mtROS has an important role in activation of NLRP3 inflammasomes and enhances production of IL- β , resulting in an inflammatory response in bMECs. Mito-TEMPO suppressed

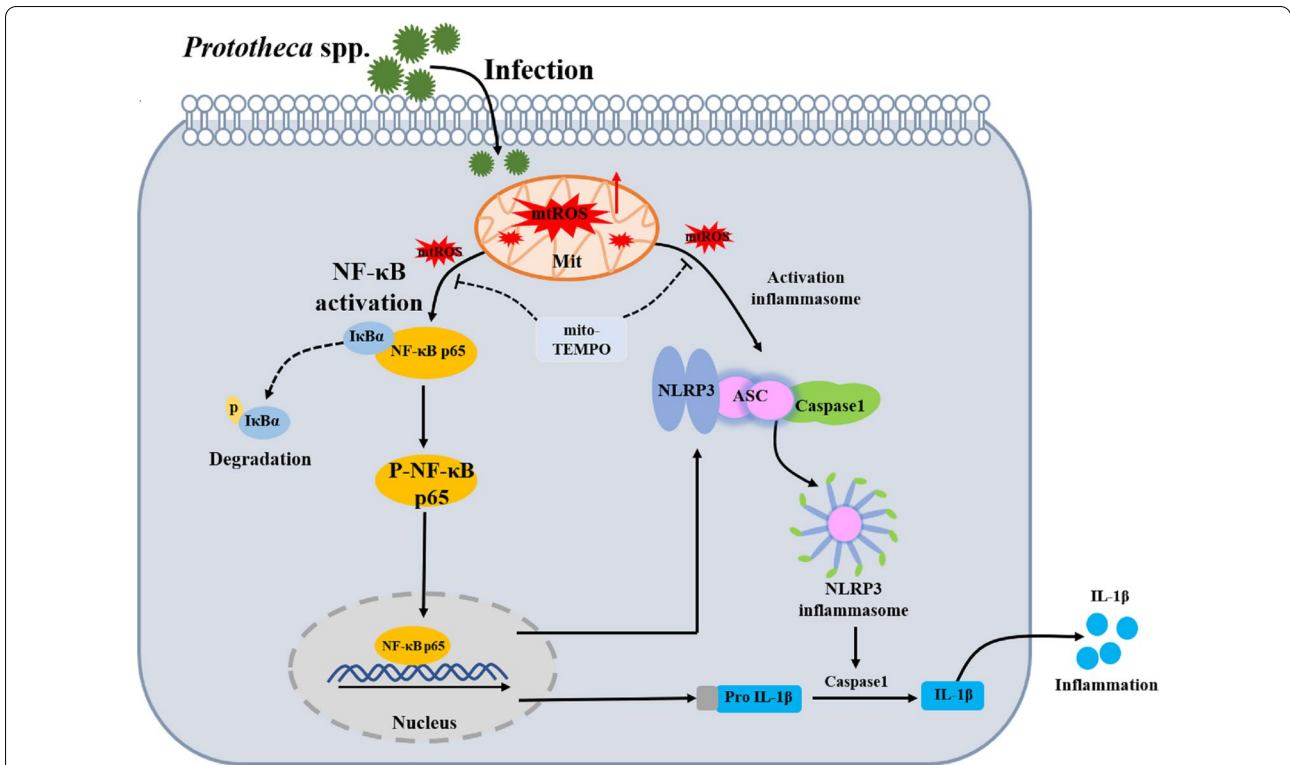


Figure 8 The pattern of *Prototheca* spp. infection induced inflammatory responses through NF-κB and NLRP3 inflammasome pathways in bMECs. Infection of bMECs with *P. bovis* or *P. ciferrii*, increased mtROS, which can promote activation of NF-κB and NLRP3 inflammasome pathways and further enhance production of IL-β, resulting in an inflammatory response in bMECs. However, in bMECs treated with mito-TEMPO, which scavenged mtROS, protein expression in NF-κB and NLRP3 inflammasome pathways was inhibited and there was suppression of the inflammatory response in *P. bovis*- or *P. ciferrii*-infected bMECs.

expression of proteins in NF-κB and NLRP3 inflammasomes pathways and reduced inflammatory responses in *P. bovis*- and *P. ciferrii*-infected bMECs (Figure 8). In this study, 3 strains in each species were randomly selected to infect bMECs. Consequently, we maximized the probability of choosing strains that represented other strains within each species in terms of pathogenicity. Regardless, mechanisms of *Prototheca* spp.-infected cells inducing mtROS generation need further study.

Infections of bMECs with either *P. bovis* or *P. ciferrii* damaged mitochondria and induced inflammatory responses, with *P. bovis* causing a more severe inflammatory response. Accumulation of mtROS had an important role in activation of NF-κB and NLRP3 inflammasomes and suppression of mtROS reduced inflammatory responses in bMECs infected with either *P. bovis* or *P. ciferrii*.

Abbreviations

bMECs: bovine mammary epithelial cells; SDA: sabouraud dextrose agar; SDB: sabouraud dextrose broth; NADPH: nicotinamide adenine dinucleotide phosphate; mtROS: mitochondrial reactive oxygen species; mito-TEMPO: mitochondrial specific antioxidant; CCK-8: Cell Counting Kit-8; BCA: Bicinchoninic

acid; RIPA: radioimmunoprecipitation assay; BSA: bovine serum albumin; DAPI: 4',6-Diamidino-2'-phenylindole dihydrochloride; PVDF: polyvinylidene difluoride; ECL: enhanced chemiluminescence; FBS: fetal bovine serum; DMEM: Dulbecco's Modified Eagle's medium; PBS: phosphate buffered solution; MOI: multiplicity of infection; TEM: transmission electron microscopy.

Supplementary Information

The online version contains supplementary material available at <https://doi.org/10.1186/s13567-021-01014-9>.

Additional file 1. The coefficient of variation values (ELISA and Real time PCR) of *P. ciferrii* and *P. bovis* infections of bMECs. The coefficient of variation (cv) is the standard deviation divided by the mean. We calculated the cv values among biological replicates within *P. bovis* and *P. ciferrii*, respectively. These cv values reflect the variation among different biological replicates and the cv values were in the range of 0.001–0.098, therefore we consider the variation among biological replicates was acceptable.

Additional file 2. The coefficient of variation values (Western blot) of *P. ciferrii* and *P. bovis* infections of bMECs. The coefficient of variation (cv) is the standard deviation divided by the mean. We calculated the cv values among biological replicates within *P. bovis* and *P. ciferrii*, respectively. These cv values reflect the variation among different biological replicates and the cv values were in the range of 0.006–0.298, therefore we consider the variation among biological replicates was acceptable.

Acknowledgements

The authors thank our laboratory members who helped us to improve the research and the manuscript with their skillful technical assistance, invaluable comments and suggestions.

Authors' contributions

BH, JG and WZ conceived and designed the experiment. WZ and FH performed the research and wrote the manuscript, WZ, FH, SX, YS and ZD performed the correlation of the genes to inflammation and associated interpretation, WZ, JG, GL, MS and ZD wrote the first draft of the manuscript. JG assisted in the result analysis and re-edited the manuscript. BH, HWB and JPK revised the manuscript. All authors read and approved the final manuscript.

Funding

This study was supported financially by: Ningxia Key R&D Project (No. 2019BBF02027), Hebei Key R&D Project (19226607D), the National Natural Science Foundation of China (No. 31572587), and the High-end Foreign Experts Recruitment Program (No. GDT20171100013).

Availability of data and materials

All data generated or analyzed during this study are included in this published article.

Declarations

Ethics approval and consent to participate

This work has received approval for research ethics from Ethical Committee of the College of Veterinary Medicine, China Agricultural University (CAU), Beijing and the study was conducted according to standard ethical guidelines implemented at CAU (SYXK, 2016-0008).

Competing interests

The authors declare that they have no competing interests.

Author details

¹Department of Clinical Veterinary Medicine, College of Veterinary Medicine, China Agricultural University, Beijing 100193, China. ²Department of Production Animal Health, Faculty of Veterinary Medicine, University of Calgary, Calgary, AB T2N 4N1, Canada. ³College of Life Sciences and Food Engineering, Hebei University of Engineering, Handan 056038, Hebei, China.

Received: 30 August 2021 Accepted: 9 November 2021

Published online: 11 December 2021

References

- Gao J, Barkema HW, Zhang L, Liu G, Deng Z, Cai L, Shan R, Zhang S, Zou J, Kastelic JP, Han B (2017) Incidence of clinical mastitis and distribution of pathogens on large Chinese dairy farms. *J Dairy Sci* 100:4797–4806
- Deng ZJ, Shahid M, Zhang LM, Gao J, Gu XL, Zhang SY, Zou J, Fanning S, Han B (2016) An investigation of the innate immune response in bovine mammary epithelial cells challenged by *Prototheca zopfii*. *Mycopathologia* 181:823–832
- Shahid M, Ali T, Zhang LM, Hou RG, Zhang SY, Ding LD, Han DD, Deng ZJ, Rahman A, Han B (2016) Characterization of *Prototheca zopfii* genotypes isolated from cases of bovine mastitis and cow barns in China. *Mycopathologia* 181:185–195
- Jagielski T, Bakula Z, Gawor J, Kr M, Kusberd WH, Dylage M, Nowakowskaf J, Gromadkab R, Karnkowskac A (2019) The genus *Prototheca* (Trebouxiophyceae, Chlorophyta) revisited: Implications from molecular taxonomic studies. *Algal Res* 43:101639
- Hirose N, Hua Z, Kato Y, Zhang Q, Li R, Nishimura K, Masuda M (2018) Molecular characterization of *Prototheca* strains isolated in China revealed the first cases of protothecosis associated with *Prototheca zopfii* genotype 1. *Med Mycol* 56:279–287
- Gao J, Zhang HQ, He JZ, He YH, Li SM, Hou RG, Wu QX, Gao Y, Han B (2012) Characterization of *Prototheca zopfii* associated with outbreak of bovine clinical mastitis in herd of Beijing, China. *Mycopathologia* 173:275–281
- Shahid M, Cavalcante PA, Knight CG, Barkema HW, Han B, Gao J, Cobo ER (2020) Murine and human cathelicidins contribute differently to hallmarks of mastitis induced by pathogenic *Prototheca bovis* algae. *Front Cell Infect Microbiol* 10:31
- Pieper L, Godkin A, Roesler U, Polleichtner A, Slavic D, Leslie KE, Kelton DF (2012) Herd characteristics and cow-level factors associated with *Prototheca* mastitis on dairy farms in Ontario, Canada. *J Dairy Sci* 95:5635–5644
- Sobukawa H, Yamaguchi S, Kano R, Ito T, Suzuki K, Onozaki M, Hasegawa A, Kamata H (2012) Short communication: molecular typing of *Prototheca zopfii* from bovine mastitis in Japan. *J Dairy Sci* 95:4442–4446
- Morandi S, Cremonesi P, Capra E, Silvetti T, Decimo M, Bianchini V, Alves AC, Costa GM, Ribeiro MG, Brasca M (2016) Molecular typing and differences in biofilm formation and antibiotic susceptibilities among *Prototheca* strains isolated in Italy and Brazil. *J Dairy Sci* 99:6436–6445
- Jagielski T, Roeske K, Bakula Z, Piech T, Wlazlo Ł, Bochniarz M, Woch P, Krukowski H (2019) A survey on the incidence of *Prototheca* mastitis in dairy herds in Lublin province, Poland. *J Dairy Sci* 102:619–628
- Bai BC, Yang YY, Wang Q, Li M, Tian C, Liu Y, Aung LHH, Li PF, Yu T, Chu XM (2020) NLRP3 inflammasome in endothelial dysfunction. *Cell Death Dis* 11:776
- Sun LB, Ma W, Gao WL, Xing YM, Chen LX, Xia ZY, Zhang ZJ, Dai ZL (2019) Propofol directly induces caspase-1-dependent macrophage pyroptosis through the NLRP3-ASC inflammasome. *Cell Death Dis* 10:542
- Petr B, Dixit VM (2016) Inflammasomes: mechanism of assembly, regulation and signalling. *Nat Rev Immunol* 16:407–420
- Missiroli S, Patergnani S, Caroccia N, Pedriali G, Perrone M, Previati M, Wieckowski MR, Giorgi C (2018) Mitochondria-associated membranes (MAMs) and inflammation. *Cell Death Dis* 9:329
- Matthew MSJ, Olhava EJ, Roush WR, Seidel HM, Glick GD, Latz E (2018) Targeting the NLRP3 inflammasome in inflammatory diseases. *Nat Rev Drug Discov* 17:588–606
- Beckwith KS, Beckwith MS, Ullmann S, Sætrea RS, Kim H, Marstad A, Åsberg SE, Strand TA, Haug M, Niederweis M, Stenmark HA, Flo TH (2020) Plasma membrane damage causes NLRP3 activation and pyroptosis during *Mycobacterium tuberculosis* infection. *Nat Commun* 11:2270
- Petr B (2016) Inflammasomes: Intracellular detection of extracellular bacteria. *Cell Res* 26:859–860
- Ma MR, Pei YF, Wang XX, Feng JX, Zhang Y, Gao MQ (2019) LncRNA XIST mediates bovine mammary epithelial cell inflammatory response via NF-κB/NLRP3 inflammasome pathway. *Cell Prolif* 52:12525
- Wu Q, Liu MC, Yang J, Wang JF, Zhu YH (2015) Lactobacillus rhamnosus GR-1 ameliorates *Escherichia coli*-induced inflammation and cell damage via attenuation of ASC-independent NLRP3 inflammasome activation. *Appl Environ Microbiol* 82:1173–1182
- Yu S, Liu XSB, Yu D, Yong EC, Yang JH (2020) Morin protects LPS-induced mastitis via inhibiting NLRP3 inflammasome and NF-κB signaling pathways. *Inflammation* 43:1293–1303
- Zhong ZY, Umemura A, Sanchez-Lopez E, Liang S, Shalpour S, Wong J, He F, Boassa D, Perkins G, Ali SR, McGeough MD, Ellisman MH, Seki E, Gustafsson AB, Hoffman HM, Diaz-Meco MT, Moscat J, Karin M (2016) NF-κB restricts inflammasome activation via elimination of damaged mitochondria. *Cell* 164:896–910
- Afonina IS, Zhong ZY, Karin M, Beyaert R (2017) Limiting inflammation—the negative regulation of NF-κB and the NLRP3 inflammasome. *Nat Immunol* 18:861–869
- Han YC, Xu XX, Tang CY, Gao P, Chen XH, Xiong XF, Yang M, Yang S, Zhu X, Yuan S, Liu F, Xiao L, Kanwar YS, Sun L (2018) Reactive oxygen species promote tubular injury in diabetic nephropathy: the role of the mitochondrial ros-txnip-nlrp3 biological axis. *Redox Biol* 16:32–46
- Xu MM, Wang L, Wang MY, Wang HY, Zhang H, Chen YQ, Wang X, Gong J, Zhang JJ, Adcock IM, Chung KF, Li F (2019) Mitochondrial ROS and NLRP3 inflammasome in acute ozone-induced murine model of airway inflammation and bronchial hyperresponsiveness. *Free Radic Res* 53:780–790
- Kim BR, Kim BJ, Kook YH, Kim BJ (2020) *Mycobacterium abscessus* infection leads to enhanced production of type 1 interferon and NLRP3 inflammasome activation in murine macrophages via mitochondrial oxidative stress. *PLoS Pathog* 16:1008294
- Zhong ZY, Liang S, Sanchez-Lopez E, He F, Shalpour S, Lin XJ, Wong J, Ding S, Seki E, Schnabl B, Hevener AL, Greenberg HB, Kisseleva T, Karin M (2018) New mitochondrial DNA synthesis enables NLRP3 inflammasome activation. *Nature* 560:198–203

28. Corbellini LG, Driemeier D, Cruz C, Dias MM, Ferreiro L (2001) Bovine mastitis due to *Prototheca zopfii*: clinical, epidemiological and pathological aspects in a Brazilian dairy herd. *Trop Anim Health Prod* 33:463–470
29. Shahid M, Cobo ER, Chen LB, Cavalcante PA, Barkema HW, Gao J, Xu S, Liu Y, Knight CG, Kastelic JP, Han B (2020) *Prototheca zopfii* genotype II induces mitochondrial apoptosis in models of bovine mastitis. *Sci Rep* 10:698
30. Jagielski T, Gawor J, Bakula Z, Decewicz P, Maciszewski K, Karnkowska A (2018) *Cytb* as a new genetic marker for differentiation of *Prototheca* species. *J Clin Microbiol* 56:e00584–e618
31. Spier A, Stavru F, Cossart P (2019) Interaction between intracellular bacterial pathogens and host cell mitochondria. *Microbiol Spectr* 7:7.2.10
32. Ramond E, Jamet A, Coureuil M, Charbit A (2019) Pivotal role of mitochondria in macrophage response to bacterial pathogens. *Front Immunol* 10:2461
33. Zavala-Alvarado C, Sismeiro O, Legendre R, Varet H, Bussotti G, Bayram J, Huete S, Rey G, Coppée JY, Picardeau M, Benaroudj N (2020) The transcriptional response of pathogenic *Leptospira* to peroxide reveals new defenses against infection-related oxidative stress. *PLoS Pathog* 16:1008904
34. Grazioli S, Pugin J (2018) Mitochondrial damage-associated molecular patterns: from inflammatory signaling to human diseases. *Front Immunol* 9:832
35. Dan Dunn JD, Alvarez LA, Zhang XZ, Soldati T (2015) Reactive oxygen species and mitochondria: a nexus of cellular homeostasis. *Redox Biol* 6:472–485
36. Guerby P, Tasta O, Swiader A, Pont F, Bujold E, Parant O, Vayssières C, Salvayre R, Negre-Salvayre A (2021) Role of oxidative stress in the dysfunction of the placental endothelial nitric oxide synthase in preeclampsia. *Redox Biol* 40:101861
37. Gaspar RS, Ferreira P, Mitchell JL, Pula G, Gibbins JM (2021) Platelet-derived extracellular vesicles express NADPH oxidase-1 (Nox-1), generate superoxide and modulate platelet function. *Free Radic Biol Med* 165:395–400
38. Ohl K, Tenbrock K (2018) Reactive oxygen species as regulators of MDSC-mediated immune suppression. *Front Immunol* 9:2499
39. Chen XL, Liu GL, Yuan YY, Wu GT, Wang SL, Yuan LW (2019) NEK7 interacts with NLRP3 to modulate the pyroptosis in inflammatory bowel disease via NF- κ B signaling. *Cell Death Dis* 10:906
40. Wang SA, Lin YK, Yuan X, Li F, Guo LX, Wu BJ (2018) REV-ERBa integrates colon clock with experimental colitis through regulation of NF- κ B/NLRP3 axis. *Nat Commun* 9:4246
41. Mulero MC, Huxford T, Ghosh G (2019) NF- κ B, I κ B, and IKK: integral components of immune system signaling. *Adv Exp Med Biol* 1172:207–226
42. Sun SC (2017) The non-canonical NF- κ B pathway in immunity and inflammation. *Nat Rev Immunol* 17:545–558
43. Zhu MM, Wang L, Yang D, Li C, Pang ST, Li XH, Li R, Yang B, Lian YP, Ma L, Lv QL, Jia XB, Feng L (2019) Wedelolactone alleviates doxorubicin-induced inflammation and oxidative stress damage of podocytes by I κ B/NF- κ B pathway. *Biomed Pharmacother* 117:109088
44. Herb M, Gluschko A, Wiegmann K, Farid A, Wolf A, Utermöhlen O, Krut O, Krönke M, Schramm M (2019) Mitochondrial reactive oxygen species enable proinflammatory signaling through disulfide linkage of NEMO. *Sci Signal* 12:5926
45. Formentini L, Santacatterina F, Núñez de Arenas C, Stamatakis K, López-Martínez D, Logan A, Fresno M, Smits R, Murphy MP, Cuezva JM (2017) Mitochondrial ROS production protects the intestine from inflammation through functional M2 macrophage polarization. *Cell Rep* 19:1202–1213
46. Man SM, Karki R, Kanneganti TD (2017) Molecular mechanisms and functions of pyroptosis, inflammatory caspases and inflammasomes in infectious diseases. *Immunol Rev* 277:61–75
47. Yang Y, Wang HN, Kouadir M, Song HH, Shi FS (2019) Recent advances in the mechanisms of NLRP3 inflammasome activation and its inhibitors. *Cell Death Dis* 10:128
48. Wang Z, Zhang SM, Xiao Y, Zhang WA, Wu SA, Qin T, Yue Y, Qian W, Li L (2020) NLRP3 inflammasome and inflammatory diseases. *Oxid Med Cell Longev* 2020:4063562
49. Kelley N, Jeltama D, Duan YH, He Y (2019) The NLRP3 inflammasome: an overview of mechanisms of activation and regulation. *Int J Mol Sci* 20:3328
50. Yu X, Lan PX, Hou XB, Han QJ, Lu N, Li T, Jiao C, Zhang J, Zhang C, Tian Z (2017) HBV inhibits LPS-induced NLRP3 inflammasome activation and IL-1 β production via suppressing the NF- κ B pathway and ROS production. *J Hepatol* 66:693–702
51. Wang XG, Eagen WJ, Lee JC (2020) Orchestration of human macrophage NLRP3 inflammasome activation by *Staphylococcus aureus* extracellular vesicles. *Proc Natl Acad Sci U S A* 117:3174–3184
52. Chung C, Chen LC, Tsang NM, Chuang WY, Liao TC, Yuan SN, OuYang CN, Ojcius DM, Wu CC, Chang YS (2020) Mitochondrial oxidative phosphorylation complex regulates NLRP3 inflammasome activation and predicts patient survival in nasopharyngeal carcinoma. *Mol Cell Proteomics* 19:142–154
53. Chung C, Yuan SN, Yang CN, Lin HC, Huang KY, Chen YJ, Chung AK, Chu CL, Ojcius DM, Chang YS, Chen LC (2018) Src-family kinase-Cbl axis negatively regulates NLRP3 inflammasome activation. *Cell Death Dis* 9:1109

Publisher's Note

Springer Nature remains neutral with regard to jurisdictional claims in published maps and institutional affiliations.

Ready to submit your research? Choose BMC and benefit from:

- fast, convenient online submission
- thorough peer review by experienced researchers in your field
- rapid publication on acceptance
- support for research data, including large and complex data types
- gold Open Access which fosters wider collaboration and increased citations
- maximum visibility for your research: over 100M website views per year

At BMC, research is always in progress.

Learn more biomedcentral.com/submissions

